

Visualization of Grain Structure in HTS HoBCO Coated Conductor Using Laser Induced Thermoelectric Voltage

Zulkifli, Zulistiana

Department of Electrical and Electronic Systems Engineering, Graduate School of Information Science and Electrical Engineering, Kyushu University : Graduate Student

Fujiwara, Takashi

Department of Electrical and Electronic Systems Engineering, Graduate School of Information Science and Electrical Engineering, Kyushu University : Graduate Student

Shoyama, Toshihiro

Department of Electrical and Electronic Systems Engineering, Graduate School of Information Science and Electrical Engineering, Kyushu University : Graduate Student

Mitsui, Daisuke

Department of Electrical and Electronic Systems Engineering, Graduate School of Information Science and Electrical Engineering, Kyushu University : Graduate Student

他

<https://doi.org/10.15017/1516861>

出版情報 : 九州大学大学院システム情報科学紀要. 11 (2), pp.91-95, 2006-09-26. Faculty of Information Science and Electrical Engineering, Kyushu University

バージョン :

権利関係 :

Visualization of Grain Structure in HTS HoBCO Coated Conductor Using Laser Induced Thermoelectric Voltage

Zulistiana ZULKIFLI*, Takashi FUJIWARA*, Toshihiro SHOYAMA*,
Daisuke MITSUI*, Takanobu KISS**, Keiji ENPUKU***,
Kazuya OHMATSU† and Yuh SHIOHARA††

(Received June 16, 2006)

Abstract: Grain structure imaging in high temperature superconductor coated conductor studies is crucial because its ability to carry current strongly depends on the microstructure. We have come with a novel method of imaging the CC grain structure using laser induced thermoelectric voltage in mm length with a resolution of 2 to 3 μm on a textured metal based HoBCO CC microbridge. Due to anisotropic difference between the ab-plane and the c-axis of the CC, we are able to visualize its grain structure at high resolution. This responsive Seebeck voltage amplitude is proportionate to the tilting angle of the CuO₂ plane of the grains relative to the tape surface. From 2D map of voltage phase signal, we can clearly visualize domain structure depending on the tilting direction of the grains. Further statistical analysis showed a good relationship with XRD crystal analysis in literature.

Keywords: High temperature superconductor, Coated conductor, Thermoelectric voltage, Seebeck constant, Grain structure, Visualization

1. Introduction

High Temperature Superconductor (HTS) has been produced for power application especially in forms of coated conductor (CC). It is produced with dimension of a few μm thickness and mm width for optimized area of current carrying capability and cost¹⁾. The usage of it for commercial use is very promising, but its complex crystal structure undeniably lead to substantial spatial inhomogeneity that becomes limiting obstacles for the super-current flow; namely grain boundaries and defects²⁾ that range from several μm to few hundred μm . These defects force the super-current to percolate around it, and cause local variations in its critical current density, J_c . It is therefore essential to study its grain structure as the J_c value is greatly influenced by the geometry and features of the CC microstructures.

This study is becoming of significance in the development of CC having the Rolling Assisted Biaxially Textured Substrates (RABiTSTM) which

consists of a biaxially metallic substrate with one or more epitaxial buffer layers having $\Delta\omega$ of 3–5°³⁾. In this sample preparation procedure, the surface condition of the substrate greatly affect the epitaxy and integrity of the buffer and superconducting layers, hence the J_c of the sample. Therefore studies in RABiTS-type conductors are of importance especially to investigate the misorientation alignment of the superconducting film with respect to the underlying substrate. It is also important to determine how narrow filaments can be made on such conductors without significant reduction in J_c , as the grains developed using this method are larger compared to other method. In this study, we utilize a novel technique to visualize the grain structure of the CC with its localized defects. Measuring its thermoelectric response due to localized variation of temperature, we succeeded to visualize the grain structure.

2. Principle of Measurement

It is well known that an electric potential will be induced as a result of local temperature gradient in solids. This is known as the Seebeck effect. The Seebeck electric potential is written as $\nabla_i \phi = S_{i,j} \nabla_j T$ where $S_{i,j}$ is the Seebeck coefficient tensor. For CC material, the Seebeck constant along ab-plane and c-axis is different; thus different thermoelectric voltage responses can be detected in each direction.

* Department of Electrical and Electronic Systems Engineering, Graduate Student

** Department of Electrical and Electronic Systems Engineering

*** Department of Superconductivity

† Sumitomo Electric Industries, Ltd.

†† Superconductivity Research Laboratory, International Superconductivity Technology Center

This phenomena generally occur in tetragonal, trigonal, hexagonal and orthorhombic crystals if the films have an orientation not along to the low-indexed crystallographic axis⁴⁾. For an example, the Seebeck coefficient difference between ab-plane and c-axis for HTS material can be as high as 7–17 μ V/K for PLD prepared YBCO on RABiTS Ni-alloy substrate. The Seebeck constants for other CC system are 0.22 μ V/K for LCMO and 3.7–7.4 μ V/K for BSCCO^{5,6)}. In early investigation of thermoelectric voltage responses on HTS samples, Testardi⁷⁾ applied a model of so-called off-diagonal thermoelectricity on a c-axis oriented YBCO at room temperature; as in **Fig. 1**. In this model, an anisotropic sample with thickness d and a tilt angle of θ with respect to the z axis, can produce the induced voltage V_x . This is proportional to the S_{xz} , the temperature gradient along z , and the heating dimension along $x(L)$ respectively; but is reversely proportional to d ;

$$V_x = \int \frac{\partial \phi}{\partial x} dx = \int S_{xz} \frac{\partial T}{\partial z} dx = S_{xz} \Delta T \left(\frac{L}{d}\right) \quad (1)$$

S_{xz} can be rewritten as $\frac{1}{2}(S_{ab} - S_c) \sin 2\theta$. Due to anisotropy, The transverse voltage induced at z direction is due to temperature change in z direction, $\frac{\partial T}{\partial z}$. Here, the transverse voltage gives information of the off-diagonal elements, where the CuO_2 planes are tilted at an angle of θ :

$$V_x = \frac{1}{2}(S_{ab} - S_c) \sin 2\theta \Delta T \left(\frac{L}{d}\right) \cong (S_{ab} - S_c) \theta \Delta T \left(\frac{L}{d}\right) \propto \theta(x, y) \quad (2)$$

From the equation, the voltage at x direction is proportional to the tilting angle. The implication of this principal to the polycrystalline CC is a responsive thermoelectric voltage amplitude which depends on the direction of the tilting angle of each domain (consisting of connected clusters of grains having the same tilting angles).

3. Sample

The HoBCO CC sample used in our experiment is prepared via in-situ pulsed laser deposition (PLD) method on an underlying RABiTS 0.1mm thick Ni alloy with $\Delta\phi$ of 9–12° and multilayer of (001) oriented $\text{CeO}_2/\text{YSZ}/\text{Ce}_2$ ⁸⁾. The buffer layers are mainly c-axis oriented. Results of the in-plane texture measurement (10m long) for each additional buffer layer, an average of $\Delta\phi$ with FWHM of 15° for YSZ (second layer) and 10° for CeO_2 as the third layer has been obtained. A general schematic of the multilayers can be seen in **Fig. 2**. We prepared a micro-bridge of

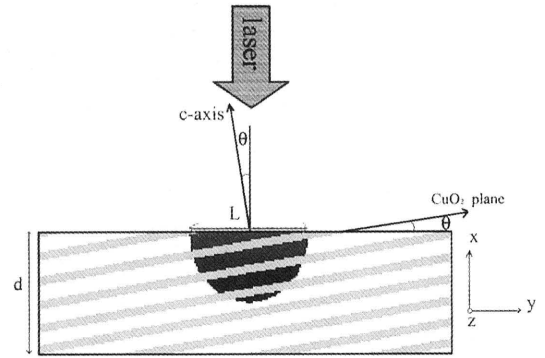


Fig. 1 Schematic orientation of the CC film with tilted CuO_2 planes.

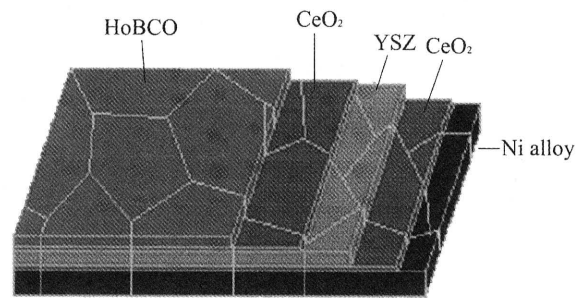


Fig. 2 Schematic diagram of HoBCO CC.

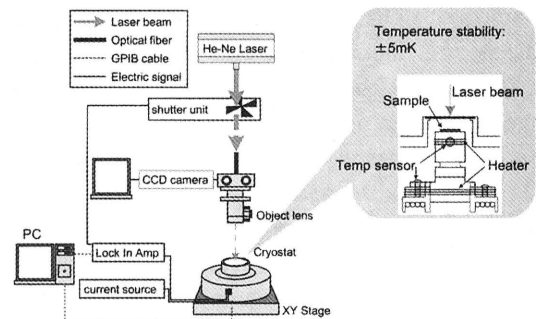


Fig. 3 Schematic diagram of the experimental setup.

200 μ m width and 1.00mm long for this study using the typical photo lithography and wet etching process. Thin copper wires are latter connected using silver paste for low ohmic resistance at both the current and voltage taps.

4. Measurements

Figure 3 shows the schematic diagram of the setup for the Low Temperature Scanning Laser Microscope (LTSLM) that we use at room temperature in this experiment. We irradiated pulsed He-Ne laser of 2.0mW at modulation frequency of 2.3kHz

using an optical chopper on top of the micro-bridge that is moved in 2D movement on a microstage. The irradiated laser induced a local thermal heating in the sample with a spot size of $2\text{--}3\mu\text{m}$, possible due to focusing of the object lens. Voltage response at each coordinate was measured using lock-in amplifier via GPIB cable to the PC while the laser beam scans the sample surface.

5. Results and Discussion

The experimental results are shown in Fig. 4(a) and Fig. 4(b). The laser irradiation induced local heating that gave rise to its thermoelectric potential locally. This potential is detected between two voltage taps at the end of the microbridge. This voltage signal changed gradually from a few nV for noise level to a few μV at some positions, thus allowing the grains and its boundaries to be seen clearly. The grain sizes were rather large, a few tens μm to hundreds of μm . This gradient change in the voltage amplitude indicated that the tilting angles change gradually, giving response to higher value as the tilting angle increased respect to the substrate planes, as in Eq. 2.

As can be seen in Fig. 4(b), phase response takes bi-stable values which shift almost 180° from each other. Histogram of the phase distribution clearly show distinct peak at -83° and $+104^\circ$. This means that the sign of the Seebeck signal changes in the domains depending on the tilt direction along the voltage terminals. Namely, the map of phase response tells us the direction of c-axis tilt in corresponding domains.

To make further analysis in a wider area, scanning of the whole bridge of the same sample was done using another bridge. Both the voltage amplitude and phase were recorded and analyzed. From the optical micrograph in Fig. 5(a), we can see that the micro-bridge are made up of grey HoBCO layer with light isolated elements at the size of a several tens μm . The results in Fig. 5(b) is a 2D map of lock-in voltage amplitude of $0\text{--}2.0\mu\text{V}$ corresponding to the position of the laser irradiation for (x, y) plane direction.

By comparison with the optical micrograph, gradient of voltage response have been recorded and relatively high voltage signals came from the light colored isolated grains indicating that these elements are some way different from the dominant aligned grains. In Fig. 5(c), we observed that the micro-bridge is made up of light blue dominant elements and yellow colored isolated clusters. The values of the

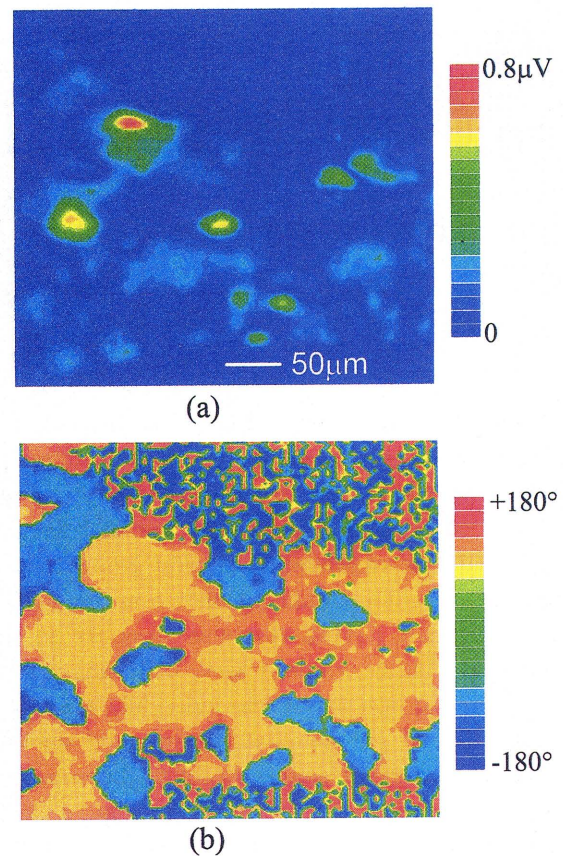


Fig. 4 Experimental result obtained in HoBCO tape deposited on a RABiTS substrate. (a) Seebeck voltage amplitude (b) phase response obtained by lock-in measurement.

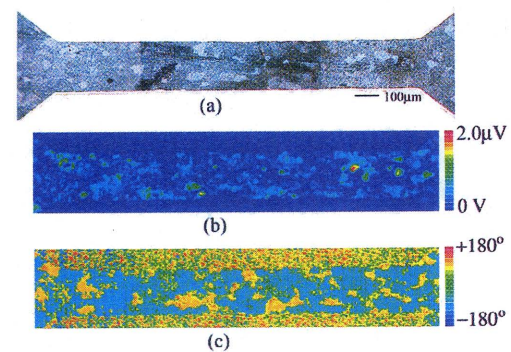


Fig. 5 (a) HoBCO CC optical micrograph (b) Seebeck voltage amplitude (c) voltage phase change.

phase change was almost constant at 180° phase, indicating there were changes in the direction of the tilting angle, giving response to either side of the voltage taps. By comparison with Fig. 5(b), the voltage phase shift occurred correspondingly to the voltage signal where we can see that the high voltage response is yellow in color.

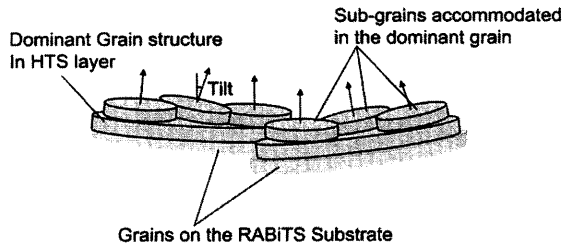


Fig. 6 Schematic diagram of grain structure in RABiTS based coated conductor.

Further investigations of Fig. 4 (a) and Fig. 4(b) showed that the phase change signified domains having distinct tilting directions. However, these domains constitutes of individual grains; therefore can actually be expanded to several grains having slight different tilting angle as shown in the voltage amplitude map, having response from nV to the maximum voltage value, $0.8\mu\text{V}$. This image also shows that on top of the big individual grain, are sub-grains that are epitaxially grown and stacked, having higher tilting angle respect to the substrate surface as schematically shown in Fig. 6. Most probably the large domain structure is originated from the textured grain on the substrate surface, which determined the tilt direction in the domain. During the deposition of HTS layer, smaller sub-grain structures are also formed at the domains, as well as the regions having well aligned CuO_2 planes.

Figure 7 is the statistical distribution of the voltage phase response. It shows that the sample has higher frequency at the negative side, making the probability at -83° is about four times higher than that at and $+104^\circ$ phase change. This suggests that instead of having the c-axis exactly parallel to the substrate, this sample shows a slight tilt to one direction.

Figure 8 is the distribution of voltage responses after taking into account the voltage sign. We can see that the distribution is of a normal pattern, having almost symmetry response on both positive and negative part. However, due to higher phase change towards the negative side, the mean value of the distribution shifts slightly to the negative side; $0.95 \times 10^{-7}\text{V}$ with the maximum peak is 1.11×10^3 and the standard deviation is $2.1 \times 10^{-7}\text{V}$ using a Gaussian fitting curve. This gives a FWHM value of $4.94 \times 10^{-7}\text{V}$. This figure represents the crystallographic information of the out-of-plane tilting $\Delta\omega$ values. Therefore, we can estimate the temperature

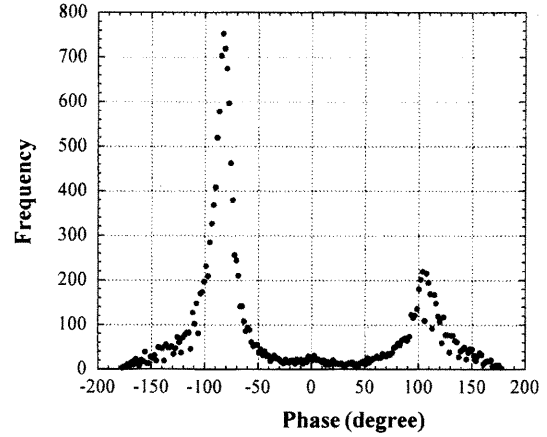


Fig. 7 Statistical distribution of voltage phase response, 180° phase difference between phase value of -83° and minor phase value of $+104^\circ$.

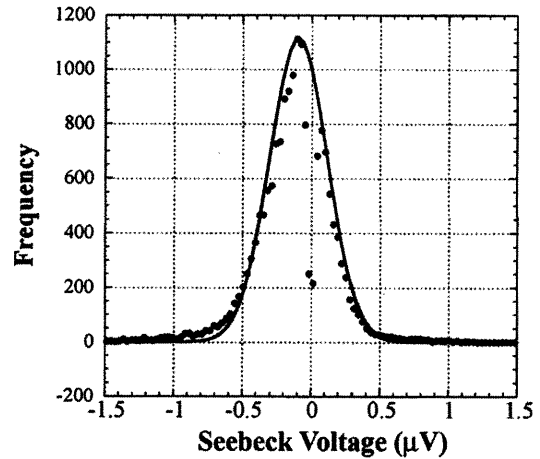


Fig. 8 Statistical distribution of the voltage signal with Gaussian fitting curve.

gradient and tilting angle from the $\Delta\omega$ in the RABiTS system. The relationship between the voltage amplitude and the $\Delta\omega$ can be written as $V = \alpha\omega$, α is the constant of $\Delta\omega$; can be rewritten as $\frac{1}{2}(S_{ab} - S_c) \sin 2\theta$ Assuming that the $\Delta\omega$ is $3-5^\circ$ as in a similar quality tape³⁾.

6. Conclusion

Using a novel method, grain structure of HoBCO based CC are able to be visualized at high resolution over a wide working area. By using laser irradiation, thermoelectricity can be induced to collect local information on the grain tilt angle at the location with spatial resolution in μm scale. From experimental results, we have managed to extract important information about the CC as compared to micrography technique. By using this technique, we

can locally feature the grains at normal state and can make estimation of the out of plane alignment. These findings are of interest especially to the production company to improve the quality of the superconducting layer and the substrate underlying it.

This technique also has high compatibility with the LTSLM²⁾ which allows us to visualize flux flow dissipation in superconducting state. Combination of those two measurements leads to deep insight to clarify the current limiting mechanism in CC. Apart from that it is also non-destructive, giving measurement at real nature of the sample. In conclusion, the crystallinity estimation and homogeneity of HTS CC can be observed at high spatial resolution and flexible working conditions, surpassing other various methods for this purpose.

7. Acknowledgements

This work was partly supported by the New Energy and Industrial Technology Development

Organization (NEDO) as Collaborative Research and Development of Fundamental Technologies for Superconductivity Applications and also supported by JSPS: KAKENHI (15360153).

References

- 1) Y. Shiohara and Y. Aoki, *Physica C*, **426-431** pp.1-7, 2005.
- 2) T. Kiss, M. Inoue, M. Yasunaga, H. Tokutomi, Y. Iijima, K. Kakimoto, T. Saitoh, Y. Tokunaga, T. Izumi and Y. Shiohara, *IEEE Trans. Appl. Supercond.*, **15** pp.3656-3659, 2005.
- 3) A. Goyal, N. Rutter, C. Cantoni and D.F. Lee, *Physica C*, **426-431** pp.1083-1090, 2005.
- 4) J. F. Nye, *Physical Properties of Crystals*, Oxford, 1985.
- 5) D. Abraimov, D. M. Feldmann, A. A. Polyanskii, A. Gurevich, G. Daniels, D. C. Larbalestier, A. P. Zhuravel and A. V. Ustinov, *Appl. Phys. Lett.*, **85** pp.2568-2570, 2004.
- 6) M. Chandra Sekhar and S.V. Suryanarayana, *Physica C*, **415** pp.1083-1090, 2005.
- 7) L. R. Testardi, *Appl. Phys. Lett.*, **64** pp.1083-1090, 2005.
- 8) S. Hahakura, K. Fujina, M. Konishi and K. Ohmatsu, *Physica C*, **412-414** pp. 931 - 936, 2004.

